lubricants

MDPI

Article

Performance of MQL and Nano-MQL Lubrication in Machining ER7 Steel for Train Wheel Applications

Kerem Yavuz Çamlı [1], Recep Demirsöz [1], Mehmet Boy [2], Mehmet Erdi Korkmaz [1,*], Nafiz Yaşar [3], Khaled Giasin [4,*] and Danil Yurievich Pimenov [5]

[1] Department of Mechanical Engineering, Karabük University, Karabük 78050, Turkey; kycamli78@gmail.com (K.Y.Ç.); recepdemirsoz@karabuk.edu.tr (R.D.)
[2] Türkiye Odalar ve Borsalar Birliği (TOBB) Vocational High School, Karabük University, Karabük 78050, Turkey; mboy@karabuk.edu.tr
[3] Yenice Vocational High School, Karabük University, Karabük 78050, Turkey; nafizyasar@karabuk.edu.tr
[4] School of Mechanical and Design Engineering, University of Portsmouth, Portsmouth PO1 3DJ, UK
[5] Department of Automated Mechanical Engineering, South Ural State University, Lenin Prosp. 76, 454080 Chelyabinsk, Russia; danil_u@rambler.ru
* Correspondence: merdikorkmaz@karabuk.edu.tr (M.E.K.); khaled.giasin@port.ac.uk (K.G.)

Abstract: In the rail industry, there are four types of steel grades used for monoblock wheels, namely ER6, ER7, ER8 and ER9. ER7 steel is manufactured in accordance with the EN13262 standard and is utilized in European railway lines. These train wheels are formed by pressing and rolling after which they are machined using turning process to achieve their final dimensions. However, machining ER7 steels can be challenging due to their high mechanical properties, which can facilitate rapid tool wear and thermal cracking. Therefore, while the use of coolants is critical to improving their machinability, using conventional flood coolants adds extra operational costs, energy and waste. An alternative is to use minimum quantity lubrication (MQL) cooling technology, which applies small amounts of coolant mixed with air to the cutting zone, leaving a near-dry machined surface. In the current study, preliminary tests were undertaken under dry conditions and using coated carbide inserts to determine the optimal cutting parameters for machining ER7 steel. The impact of the cutting speed and feed rate on surface roughness (R_a), energy consumption and cutting temperature were investigated and used as a benchmark to determine the optimal cutting parameters. Next, additional machining tests were conducted using MQL and nano-MQL cooling technologies to determine their impact on the aforementioned machining outputs. According to preliminary tests, and within the tested range of the cutting parameters, using a cutting speed of 300 m/min and a feed rate of 0.15 mm/rev resulted in minimal surface roughness. As a result, using these optimal cutting parameters with MQL and Nano-MQL (NMQL) cooling technologies, the surface roughness was further reduced by 24% and 34%, respectively, in comparison to dry conditions. Additionally, tool wear was reduced by 34.1% and 37.6%, respectively. The overall results from this study demonstrated the feasibility of using MQL coolants as a sustainable machining alternative for steel parts for rail wheel applications. In addition, the current study highlight the enhanced performance of MQL cooling technology with the addition of nano additives.

Keywords: ER7 steel; nano-MQL; machinability; surface roughness; tool wear

Citation: Çamlı, K.Y.; Demirsöz, R.; Boy, M.; Korkmaz, M.E.; Yaşar, N.; Giasin, K.; Pimenov, D.Y. Performance of MQL and Nano-MQL Lubrication in Machining ER7 Steel for Train Wheel Applications. *Lubricants* **2022**, *10*, 48. https://doi.org/10.3390/lubricants10040048

Received: 25 February 2022
Accepted: 20 March 2022
Published: 23 March 2022

1. Introduction

Train wheels are produced as a single piece from low-alloyed carbon steel grades such as ER7 steel [1]. In the heat treatment stage, the train wheel is heated up to 830 °C and then cooled to 200–230 °C for hardening. Then, the hardened material is kept for 1–2 h before it is tempered at 530 °C for 3 h [2]. Wheel rail components should possess wear and corrosion resistance characteristics since they are continuously subjected to static and dynamic loads [3]. For this reason, material properties such as the type of alloying

elements added to the material, production method and heat treatment have a direct impact on the quality of the train wheels. Moreover, the expected surface quality of a train wheel produced with ER7 material after machining is very high (0.8–3.2 μm) [4]. Therefore, understanding the machinability of ER7 steel is critical to ensuring that the machined wheels meet the stringent surface finish requirements. Therefore, past studies in the open literature investigated the wear behavior, heat treatment and microstructural changes of steel alloys used in the rail industry. The studies employed a combination of surface microstructure techniques such as LSCM, SEM, EBSD, TEM and X-ray diffraction. Hu et al. [1] studied the microstructures, and differences in the microstructures, of three different types of railway wheel materials (ER7, CL60 and C grade) with varying ferrite content (XRD). There was also a discussion about the link between fatigue and wear. In another work by Hu et al. [5], the wear behavior of five different wheels and four different rail material pairings with varying hardness values was investigated. They discovered that when the hardness of the wheels and rails increased, the wear rate reduced and then marginally increased. There were significantly fewer cracks found on PG4 and PG5 rails according to their analysis of the five wheel materials. In another study, Hu et al. [6] also observed that, as the wheel and rail hardness ratios increased, the wheel wear rate decreased but the rail wear rate increased. They observed that low fatigue wear turns into severe fragmentation and severe fatigue wear as the void rate increases with decreasing hardness values for both materials. Angelo et al. [7] reported that double-disc tests on rail steel specimens exposed to dry contact with cast iron brake block specimens, dry contact with rail steel specimens and wet contact with rail steel specimens matched the braking effect while minimizing the damage to the ER7 steel railway wheels. Additionally, nondestructive testing procedures (weight loss, surface temperature and coefficient of friction) were employed to inspect material structures. According to their results, the most important mechanism of damage is the expansion of the surface fracture caused by the pressure of the liquids in wet contact. They employed FEA (finite element analysis) to determine the stress intensity factor (SIF) applied at the tip of the surface crack and the propagation limit of these cracks, which are critical requirements for damage avoidance. T. Giętka and K. Ciechacki [8] focused on the real load values and material behavior, not only measuring on a test or real object, but also simulating and analyzing them with FEA for verification. They stated that the material they proposed in their study met the criteria specified in the light of the literature review and the simulation results obtained. As a result, they stated that ADI (austempered ductile iron) material is 20.7% more advantageous than monoblock material based on the analysis of the mass difference. In addition, there a rich literature which investigated the effect of coatings on reducing the surface defects and wear in wheel train made from ER7 steel experimentally and numerically [9–11]. However, limited studies can be found in the open literature on the machinability of the train wheels made from ER7 steel. Increasing global competition stimulated businesses to produce high-quality and low-cost products which made it mandatory for enterprises to choose the appropriate machining parameters to produce the desired qualities in the machined parts [12,13]. If the appropriate parameters are not selected, rapid wear, breakage and deformations might occur in the cutting tools, deteriorating the surface quality of the machined parts which in return will have an adverse effect on the cost and quality [14]. In parallel with technological developments, different cutting fluids are currently being used in machining hard-to-cut materials [15,16]. These cutting fluids are sometimes embedded with additives according to the machined material and manufacturing conditions [17–19]. Although cutting fluids can improve the machining process, they may have negative effects on the environment (disposal and recycling) and human health (skin irritation). To minimize the negative effects of cutting fluids, minimum quantity lubrication techniques were developed which use small amounts of coolants mixed with air to reduce the amount of fluid used during the machining process [20,21].

Obikawa et al. [22] observed that, when machining carbon steel, MQL was more effective in reducing nose and flank wear than a solution type cutting fluid. Dniz et al. [23]

evaluated the influence of MQL and other cooling strategies on the machinability of AISI 52100 steel using various types of cutting tool materials. Their findings indicated that traditional coolant machining resulted in increased tool wear and decreased surface roughness when compared to dry and MQL machining settings. Unlike many previous studies that compared the MQL technique to the dry, standard coolant and compressed air, this study recommends MQL turning for improved surface roughness and reduced tool wear. Dhar et al. [24] evaluated the effects of turning AISI 1040 steel on cutting temperature, chip shape and dimensional accuracy in another investigation, comparing the MQL approach to the dry and standard coolant. According to the experimental data, MQL can significantly reduce the cutting temperature and dimensional error rates at various cutting speeds and feed rates. MQL leaves a near-dry machined surface and can reduce the cutting temperature at the tool–chip interface more than other types of cooling techniques due to the better penetration of the lubricant with the assistance of pressurized air [25–28]. In addition, chip breakability and separation were improved using MQL due to the effective lubrication and the ability of the pressurized air to blow cut chips away from the cutting zone [29]. To increase the efficiency of MQL cooling systems and to improve the tribological properties, the use of nanofluids by adding nanolubricants and nanoparticles is becoming increasingly common. Yildirim et al. [30] compared the results obtained with dry and pure MQL by adding hBN nanoparticles with a low coefficient of friction and excellent lubricating properties at two different rates (0.5 and 1 vol%). They stated that the best machining output results were obtained with nano-MQL. Moreover, 0.5%-hBN-added MQL showed a 43% improved performance on tool wear, while 1%-hBN-added MQL showed approximately a 30% improved performance on the cutting temperature than the dry condition. The authors also stated in another study that hBN-added nanoparticles have a positive effect on the milling process as well as on the machining outputs [31]. Additionally, Nguyen et al. [32], from their tribometer tests, stated that hBN particles are effective in reducing flank and central wear. Similarly, previous studies reported that adding hBN nanoparticles in the coolant improved the quality of the machined parts [33–35]. Different nanosolid-added lubricants (silicon carbide, Al_2O_3, carbon, carbon derivatives, graphene, etc.) had a positive impact on the overall machining process [36,37]. Pandey et al. [38] evaluated the chip morphology and tool wear using two different nano-MQL methods and found that using CNT (carbon nanotubes)-based NFMQL performed better than alumina-based NFMQL (nanofluid minimum quantity lubrication). Chetan et al. [39] analyzed the machinability of nickel alloy using cooling and lubrication with nano-MQL (Al_2O_3 nanoparticle addition), cryogenic cooling (CC) and cryogenic treatment (CT). Their results showed that using nano-MQL reduced the cutting forces by 16%, while machining with CC was more effective in cutting edge wear.

The results of a comprehensive assessment of the relevant literature suggest that there is not a single study on the machinability of the ER7 train wheels when the final product is produced utilizing turning, milling or drilling operations after they have been manufactured. This lack of literature, together with the rising frequency of rail transportation networks around the globe, demonstrates the significance of the ER7 material's machinability. In addition, the impact of cutting tools on the prices of machinability is a crucial consideration to keep in mind. To fill this gap in the literature, the purpose of this research is to find the optimal values of the cutting parameters (feed rate and cutting speed) in the first stage, and the influence of the optimal cutting parameters on tool life under dry, MQL and nano-MQL conditions in the second and final stages of the investigation.

2. Materials and Methods

EN 13262 standard is used to determine the characteristics of train wheels used in European railway networks. In this standard, four different steel grades, ER6, ER7, ER8 and ER9, are defined for use in train wheels. These grades have low carbon content (0.55% C) and pearlitic and ferritic structures. ER6 and ER7 steel grades are generally used as a wagon wheel material. After the train wheels are produced by the forging process,

they are processed on special vertical CNC (Computer Numerical Control) lathes due to their geometric shape, size and weight. Since there is not enough lathe in size for the machining of the commercially produced train wheels in the university laboratories, ER7-quality material with the dimensions of 170 × 50 mm was taken from the wheel hub to be used as a test workpiece. The chemical composition of the ER7-quality steel used in turning experiments is shown in Table 1. The ER7 steel samples used in the current study were obtained from Kardemir Inc. (Sanayi Karabuk, Turkey), which manufactures and commercially sells train wheels.

Table 1. The chemical composition of ER7 steel (wt%).

C	Mn	Si	S	P	Cr
0.52	0.80	0.40	0.015	0.020	0.30
Ni	**Cu**	**Mo**	**V**	**Cr + Ni + Mo**	**H.ppm**
0.30	0.30	0.080	0.060	0.50 max	2.0 max

In the experiments, CNMG 120408 P20-quality tools and suitable tool holders were used as per the ISO standards of the Korloy company. Karabük University's TTC-550 CNC lathe was used for the tests. In the preliminary studies, a fixed cut depth of 1 mm, three different cutting speeds (200, 250, 300 m/min) and three different feed rates (0.15, 0.20, 0.30 mm/rev) were all employed together according to the cutting tool manufacturers and the industry recommendations. The depth of cut is directly proportional to the MRR during turning. Due to the keeping constant of the MRR (or cutting length), the depth of cut is kept constant at 1 mm. The temperatures on the cutting tool and workpiece during turning were measured with the Fluke TI400 infrared camera. The infrared camera has automatic focusing, a temperature measuring range of 0 °C to 1200 °C and a measurement accuracy of ±2 °C. The KAEL network analyzer with three 60/5A current transformers was used to precisely measure the power consumption of the CNC lathe during turning. After each machining parameter, the surface roughness of the workpiece was measured with the Mahr M300 roughness device. For each measurement, the workpiece was rotated approximately 72°, measured from five different regions and evaluated by taking the average value. The experimental setup is shown in Figure 1.

Dry, MQL and nano-MQL were also used to determine the optimal conditions after the optimum parameters were determined from the preliminary turning tests. It was supplied by the SBH Company (Istanbul, Turkey) and used an MQL system by Werte. The cutting fluid (WerteMist) was distributed in two dimensions by an additional air pump fitted by the manufacturer. The MQL system made use of WerteMist (Table 2), a volatile proprietary lubricant. Next, 40 to 50 nm-sized nano-hBN particles were mixed into a commercial vegetable cutting liquid at a weight ratio of 1% (WerteMist). Using the Hydra ultrasonic stirrer, the produced liquid was agitated for an hour to reduce nanoparticle clumping. A magnetic stirrer, developed by MTops MS300HS, was also employed to improve the homogeneity of nanoparticles with the cutting fluid (Figure 2). To ensure that the air pressure used was maintained at 5 bar, a manometer was used. In all cooling settings, the flow rate was 100 mL/hr. Quality properties such as roughness (R_a), power consumption (W) and temperature (°C) were used in an experimental design. Cutting speed (V) and feed rate (F) were found to be the main regulating elements. Analysis of variance (ANOVA) was performed to explore the influence of the input parameters and their interactions on the measured outputs using Minitab 17 software.

Table 2. Properties of the MQL coolants used in the machining experiments.

Property	MQL	Nano-MQL
Density (kg/m^3)	0.9	0.92
Kinematic viscosity (mm^2/s) @ 40 °C	5.3	2.7
Nanoadditive particles	—	hBN
Nanovolume concentration	—	1%
Nozzle pressure (bar)	5.0	5.0

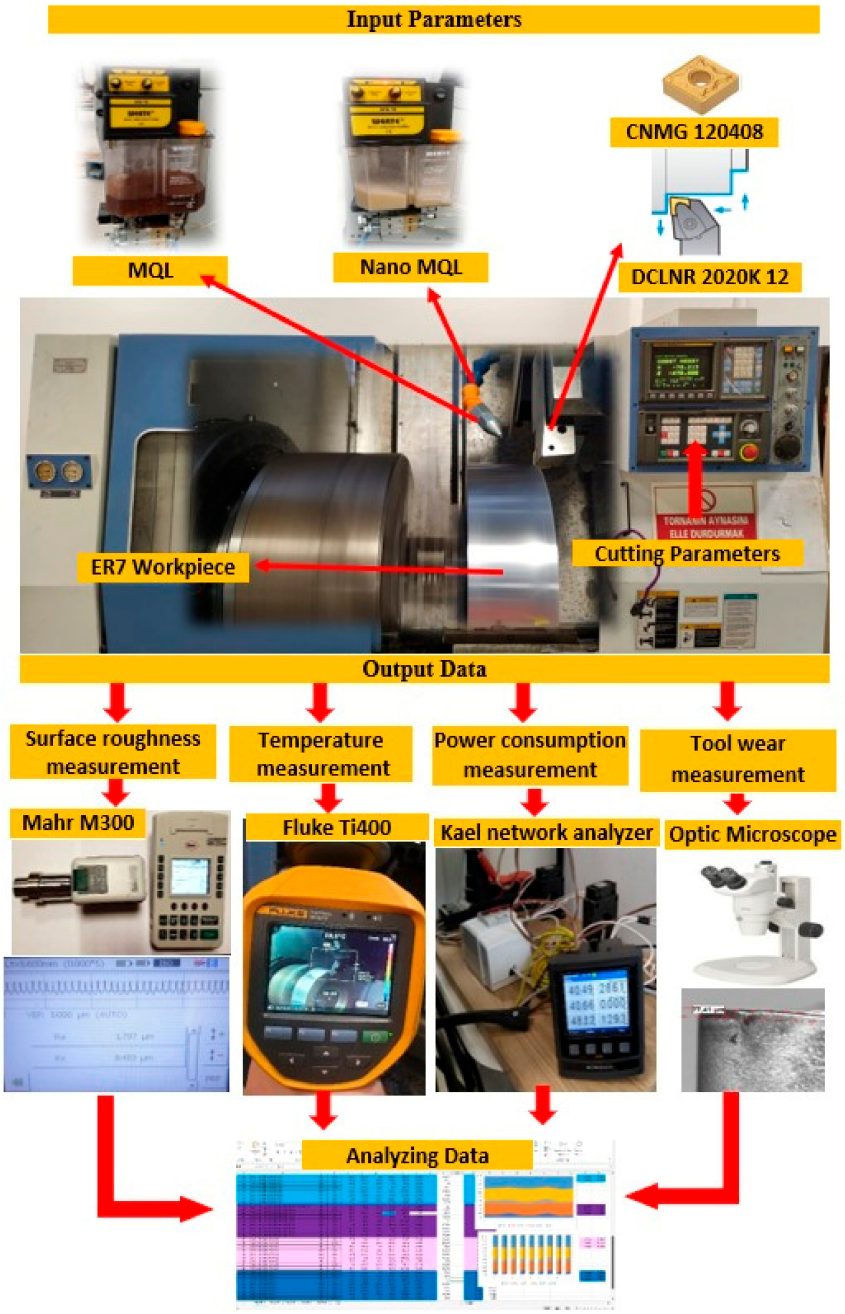

Figure 1. Experimental setup.

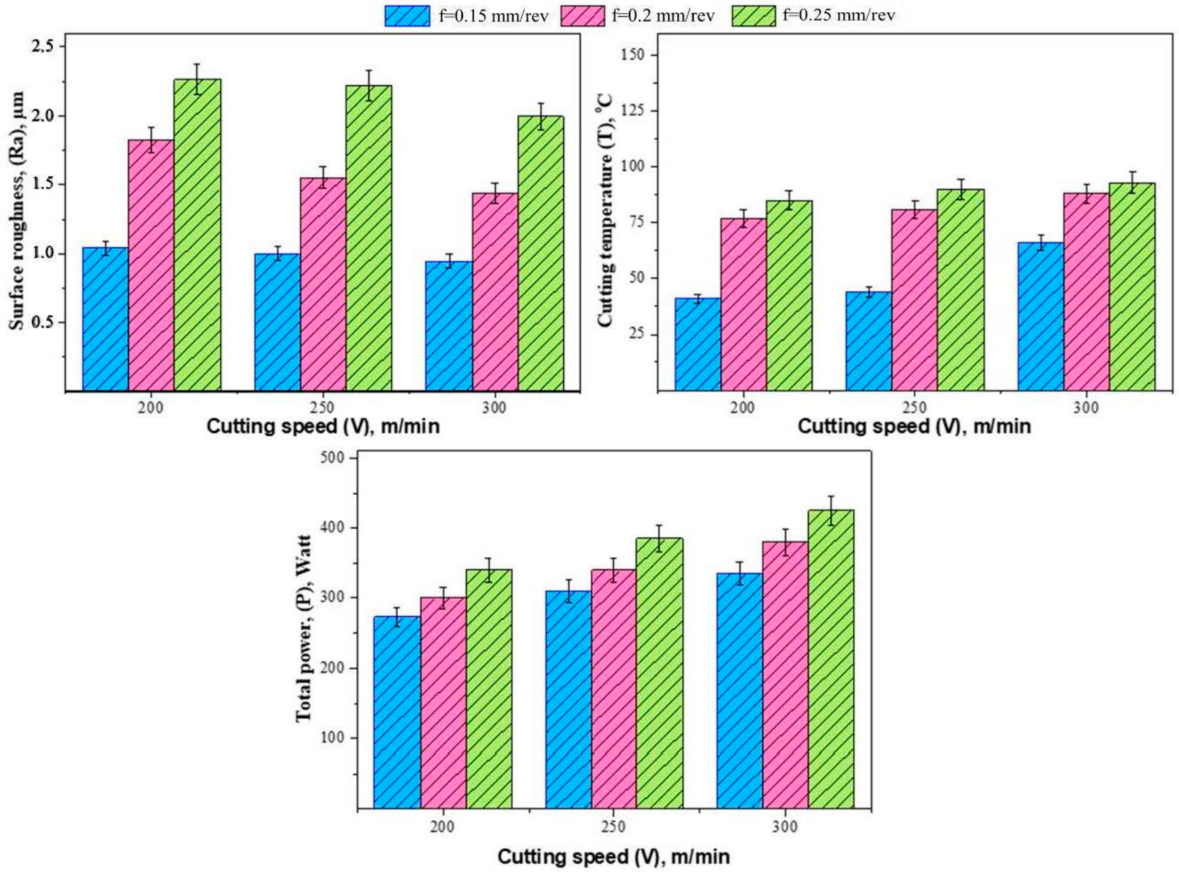

Figure 2. The effect of cutting parameters on for surface roughness, cutting temperature and total power consumption.

3. Results and Discussion

3.1. Preliminary Experiments

Three different cutting speeds and feed rates were employed in the preliminary tests. Table 3 summarizes the surface roughness, power consumption and machining temperature at different cutting parameters.

Table 3. Cutting parameters levels and the resulting outputs (optimum cutting parameters are in bold).

Exp. No.	Cutting Speed (V-m/min)	Feed Rate (f-mm/rev)	Surface Roughness (R_a-µm)	Total Power (W)	Temperature (°C)
1	200	0.15	1.040	273.3	41
2	200	0.2	1.828	300.3	77
3	200	0.25	2.264	340.3	85
4	250	0.15	0.999	310.3	44
5	250	0.2	1.554	340.3	81
6	250	0.25	2.168	385.3	90
7	**300**	**0.15**	**0.946**	**335.3**	**66**
8	300	0.2	1.439	380.3	88
9	300	0.25	1.996	425.3	93

In Figure 2, the machining outputs (surface roughness, cutting temperature and power consumption) of the test experiments are given. The total power consumption measured during the machining process was obtained from the sum of the linear power, idle mode power, spindle power and machining power outputs. The mechanical energy is transferred

to thermal energy in practically all machining processes. According to Figure 2a, the maximum surface roughness was achieved at 200 m/min and 0.25 mm/rev. The lowest surface roughness was achieved at 300 m/min and 0.15 mm/rev. When the feed rate was increased from 0.15 to 0.20 mm/rev or from 0.15 to 0.25 mm/rev, the surface roughness increased by 52.11% and 111%, respectively, which was mainly due to increased uncut chip thickness. The machined workpiece has surface roughness values of 0.946, 1.440 and 1.996 m, respectively, and rising values of 52.11% and 110%. The surface roughness was 1.828, 1.554 and 1.439 µm at the feed rate of 0.20 mm/rev and at the cutting speed of 200, 250 and 300 m/mi, respectively. When the cutting speed was increased from 200 to 250 m/min or 200 to 300 m/min, the surface roughness was reduced by 14.99% and 21.28%, respectively. Table 4 shows the *p*-value and percentage contribution (PCR) results from the ANOVA tables of the analyzed outputs. The significant parameters and their interactions are highlighted in blue (according to *p*-value < 0.05) [40,41]. From the table, it can be seen that the feed rate was the was the most significant cutting parameter on the surface roughness, with 94.087%, followed by the cutting speed, with 4.485%. The linear interactions between the cutting speed and the feed rate were insignificant. Therefore, the cutting parameters which provide the lowest surface roughness are 300 m/min and 0.15 mm/rev, taking into account that—according to the ANOVA results—it is expected that the feed rate would have a significant effect on the machining outputs for the MQL tests in the main part of the study.

Table 4. ANOVA results for surface roughness, cutting temperature and power consumption in preliminary tests (signficant interactions are in bold).

	Surface Roughness		**Cutting Temperature**		**Power Consumption**	
Source	***p*-Value**	**PCR (%)**	***p*-Value**	**PCR (%)**	***p*-Value**	**PCR (%)**
Cutting Speed—V (m/min)	0.0310	4.485	0.022	10.597	0.00007	48.311
Feed Rate—f (mm/rev)	0.0004	**94.087**	0.001	**74.929**	0.00007	**50.463**
V × V	0.8440	0.014	0.333	0.730	0.26813	0.091
F × f	0.5500	0.138	0.025	9.723	0.11164	0.245
V × f	0.3560	0.362	0.129	2.373	0.03008	0.744
Error		0.915		1.648		0.147
Total		100		100		100

According to Figure 2b, the highest cutting temperature occurred at 300 m/min and 0.25 mm/rev and lowest at 200 m/min and 0.15 mm. The cutting temperature increased with the increase of the cutting speed (due to the increased rubbing between the tool and workpiece) and with the increase of the feed rate (due to the increased chip load). It is known that the tool life deteriorates as the cutting temperatures rise during the cutting process. The cutting temperature recorded at 300 m/min and 0.15 mm/rev was 66 °C, 88 °C at 0.20 mm/min and 93 °C at 0.25 mm/rev. The cutting temperature increased by 33.3% and 40.9%, respectively, when the feed rate was increased from 0.15 to 0.20 mm/rev and 0.15 to 0.25 mm/rev. The cutting temperature values of 85 °C, 90 °C and 93 °C were obtained with a feed rate of 0.25 mm/rev and a cutting speed of 200 m/min, respectively. When the cutting speed was increased from 200 to 250 m/min or 200 to 300 m/min, the temperature increased by 5.88% and 9.41%, respectively. The analysis of variance for temperature is given in Table 4. When the values are examined, it is seen that the effective parameter is the feed rate, which was about seven times higher (74.929%) than that of the cutting speed (10.597%). As a result, to attain lower machining temperatures, it is recommended to use a cutting speed of 200 m/min and a feed rate of 0.15 mm/rev. The error values can be explained by the presence of other variables, which were not considered in this study, such as bench vibrations, floor vibrations or the microstructure of the material. These error values were calculated as 1.648%.

The overall power output was determined at various cutting speeds and feed rates. Reduced power consumption was achieved through higher cutting speeds and lower feed

rates. Furthermore, the lowest power consumption was observed when cutting at a speed of 200 m/min and feeding at a rate of 0.15 mm/rev. At a cutting speed of 300 m/min and a feed rate of 0.15 mm/rev, the graph in Figure 2c indicates a power consumption of 335.3 W; at a feed rate of 0.20 mm/rev, the power consumption increases to 380.3 W. It measured 425.3 W at a cutting speed of 300 m/min and a feed rate of 0.25 mm/rev. Increases in power consumption of 13.42% and 26.84%, respectively, occur when the feed rate value is increased from 0.15 mm/rev to 0.20 mm/rev and from 0.15 mm/rev to 0.25 mm/rev. The CNMG cutting tool utilized 340.3 W of power at a feed rate of 0.25 mm/rev at a cutting speed of 200 m/min, 385.3 W at a cutting speed of 250 m/min and 425.3 W at a cutting speed of 300 m/min. When cutting speeds are increased from 200 m/min to 250 m/min or 300 m/min, power consumption increases by 13.22% and 24.98%, respectively. The ANOVA results for power consumption are given in Table 4. When the values are examined, it is seen that the effective parameter is the feed rate. The PCR of feed rate is approximately 2% higher than the PCR of the cutting speed parameter. While the effective rate of the feed rate was 50.46%, the effect of cutting speed was found to be 48.311%. Again, the cutting speed and feed rate values are also statistically significant. As a result, for a lower energy consumption, a combination of 200 m/min and 0.15 mm/rev is recommended. However, from the preliminary test results, a set of cutting parameters (highlighted in blue) which provide the optimal (lowest) surface roughness was chosen for the MQL and nano-MQL tests. This is because the surface roughness is considered as the most important factor for the performance of the train wheel during its service.

3.2. MQL and Nano-MQL Experiments Analysis

In this study, turning experiments were carried out under different machining conditions, taking into account the optimum values of the cutting parameters used in dry cutting conditions. When the maximum flank wear reached 0.2 mm [42], the tool performance was evaluated. Figure 3 shows the variation of tool wear depending on machining conditions and cutting length.

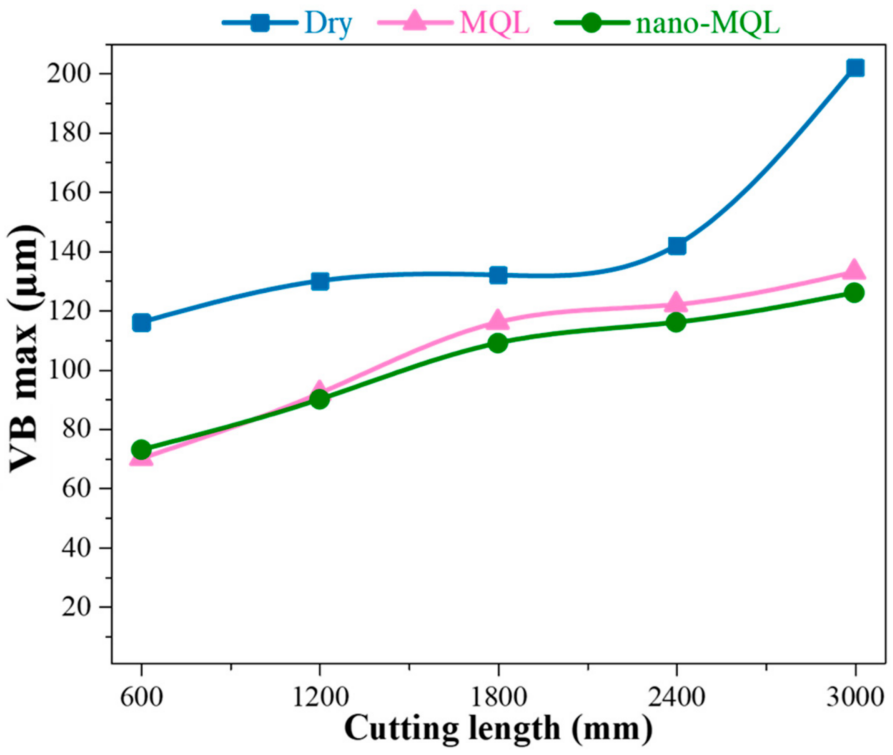

Figure 3. Variable of flank wear in V_c = 300 m/min and f = 0.15 mm/rev.

It is seen from Figure 3 that the flank wear (VB) increases in all variables depending on the increasing cutting length, which is an expected situation. In the wear mechanism, which was measured in five stages, the highest amount was obtained in dry cutting conditions, with 116 µm in the first measurements. In the experiments carried out with MQL and nano-MQL, wear of 70 and 73 µm occurred, respectively. Although the rate of change in the amount of wear was higher in the experiments performed with MQL and nano-MQL compared to the fourth stage measurements, there was a rapid deterioration of the tool life in the test performed under dry cutting conditions in the fifth stage, and the targeted wear amount (0.2 mm) was reached. This can be explained by the higher temperature values that occur under dry processing conditions. Considering the last stage, it is possible to say that the highest tool performance is obtained in nano-MQL, and the lowest tool performance is obtained in dry cutting conditions. To express this situation proportionally, it is seen that the MQL and nano-MQL applications applied depending on the cutting length have a better performance of approximately 34.1% and 37.6%, respectively, in the VB value in the last stage measurements compared to the dry cutting conditions. It is known that coolants form a wear-retarding thin film layer at the cutting tool–workpiece contact in machining processes. In addition, it can be said that the decrease in temperatures in the cutting zone delays tool wear [43]. These conditions can be explained by the fact that the machining conditions performed with MQL give better results than dry machining. It is understood from the results that nano-MQL processing obtained by adding nanosolid lubricant is more efficient than other processing conditions. This can be explained by the fact that nano additives cause better lubrication in the cutting zone and thus lower cutting temperatures [44]. It is known that cutting tool costs have an important place in machining operations in terms of costs, and it is possible to say that machining with nano-MQL and MQL is more suitable than dry machining in terms of efficiency. In addition, when the MQL method is used with environmentally friendly cutting oils, it is very safe in terms of employee health and the environment [45]. These oils are consumed by evaporation with the heat generated between the cutting tool and the workpiece without the need for an extra process. The flank and crater wear images formed on the cutting tool as a result of the experiments are given in Figure 4.

The surface roughness (R_a), which is the machining output, varies depending on many parameters (cutting speed, feed rate, depth of cut, cutting tool material, etc.). Figure 5 shows the variation of R_a values according to the machining conditions at different machining lengths. Compared to dry machining conditions, it is evident that lubrication methods play an important role in achieving a better surface finish (Figure 5). In the first stage of measurements, the highest R_a value was obtained as 1.05 µm in dry machining conditions. Compared with the same conditions, it is seen that the result obtained with MQL is approximately 24%, and the result obtained with nano-MQL is approximately 34% lower. The MQL application provides better surface quality because it reduces the contact and friction between the tool–workpiece pair. In addition to good lubrication in the cutting zone, nanoparticles have good thermal conductivity and can efficiently remove heat from the cutting zone, therefore improving the surface quality [46]. A similar upward trend is observed for each processing condition until the final stage measurements. This was expected and can be explained by the increased amount of wear [47], as seen from Figure 3. Since the nose radius of the cutting tool is also a cutting parameter that affects the surface roughness, the increased amount of wear directly affects R_a. The nano-MQL application seems to be effective in obtaining the most efficient outcomes based on surface quality, including in the wear mechanism [48]. To better understand the surface quality, Optical and 3D surface images are given in Figure 6.

Figure 7 shows the power consumption values at different machining lengths according to different machining conditions. The power consumption results show a similar trend with the R_a and VB results. The highest power consumption occurred in dry machining conditions. It was approximately 345 W for the first stage and approximately 355 W due to tool wear in the final stage. Considering the first stage values, the power consumption

of the MQL application is approximately 5.5% less. Compared to the nano-MQL system, this decrease was approximately 7.7%. In addition, since the sum of the powers obtained at each stage is considered, it has been calculated that there is approximately 5.3% and 10.2% lower power consumption in the experiments performed with MQL and nano-MQL, respectively. This can be explained by the fact that the MQL and nano-MQL systems can reduce the friction between the tool and the workpiece depending on the layer formed, and, accordingly, the power consumption decreases, as illustrated by Gupta et al. [49] and Korkmaz et al. [50]. In the light of these results, it can be said that the MQL and nano-MQL systems are effective in terms of energy efficiency and sustainability.

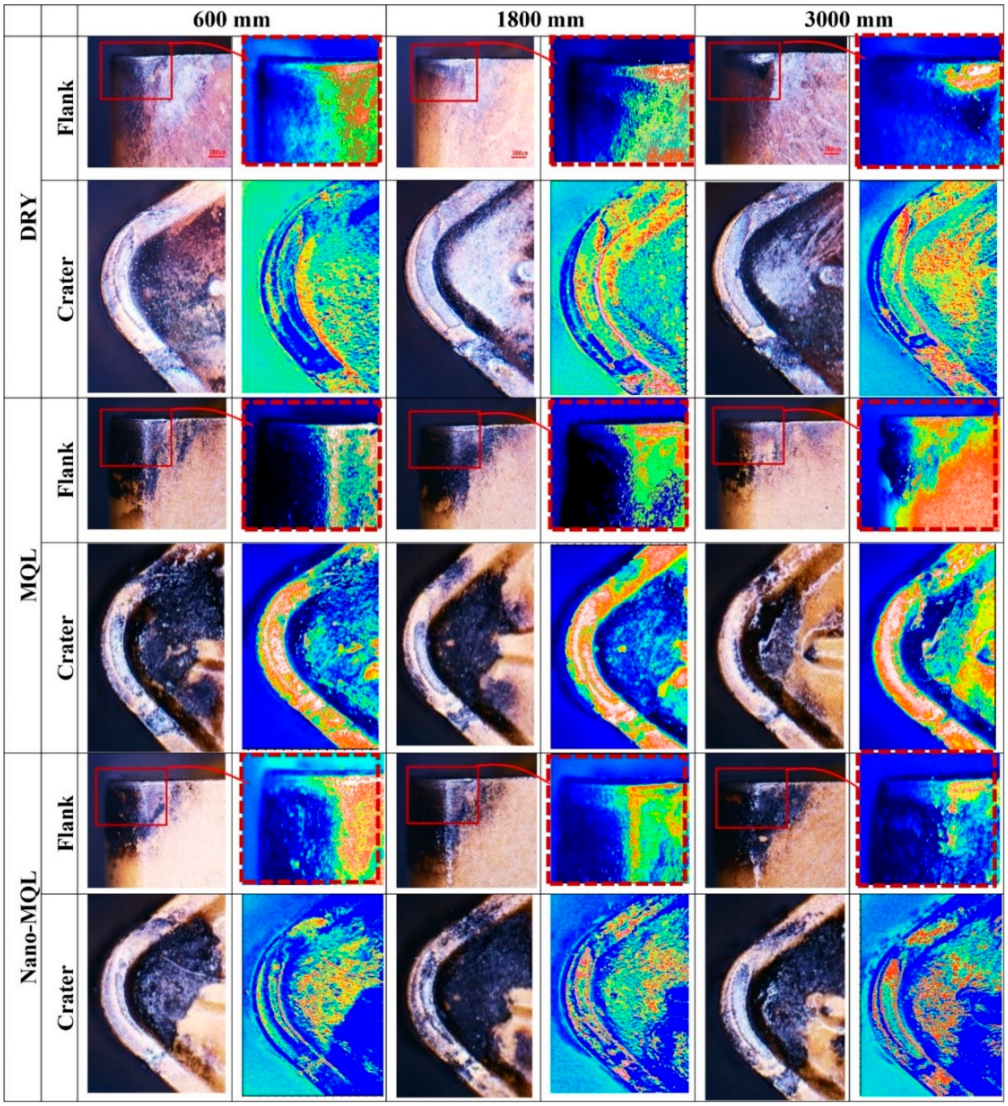

Figure 4. The cutting tool wear images under different cutting conditions.

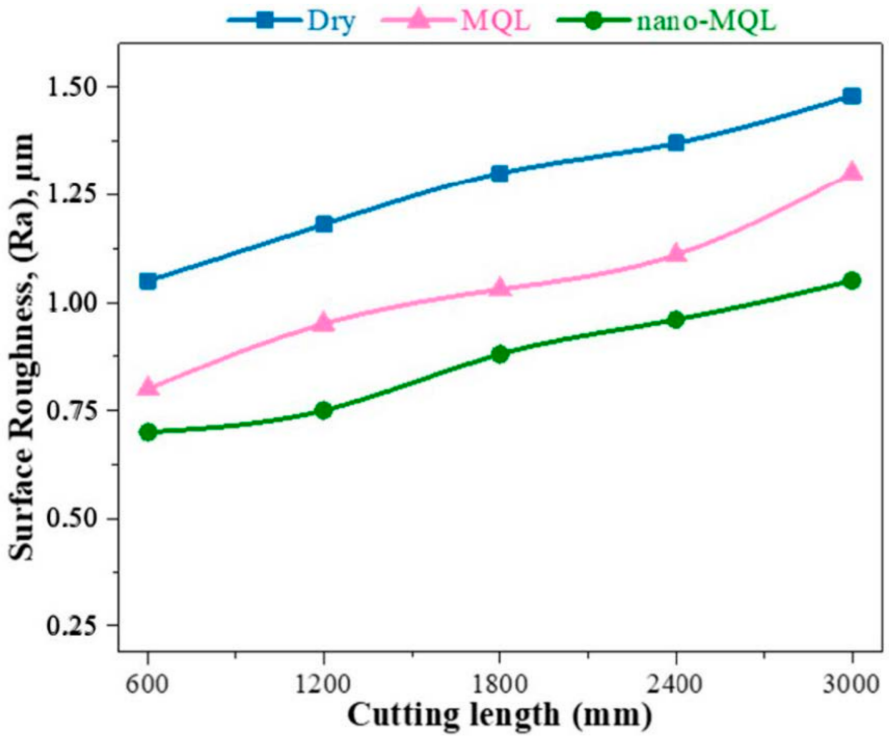

Figure 5. Variable of surface roughness in V_c = 300 m/min and f = 0.15 mm/rev.

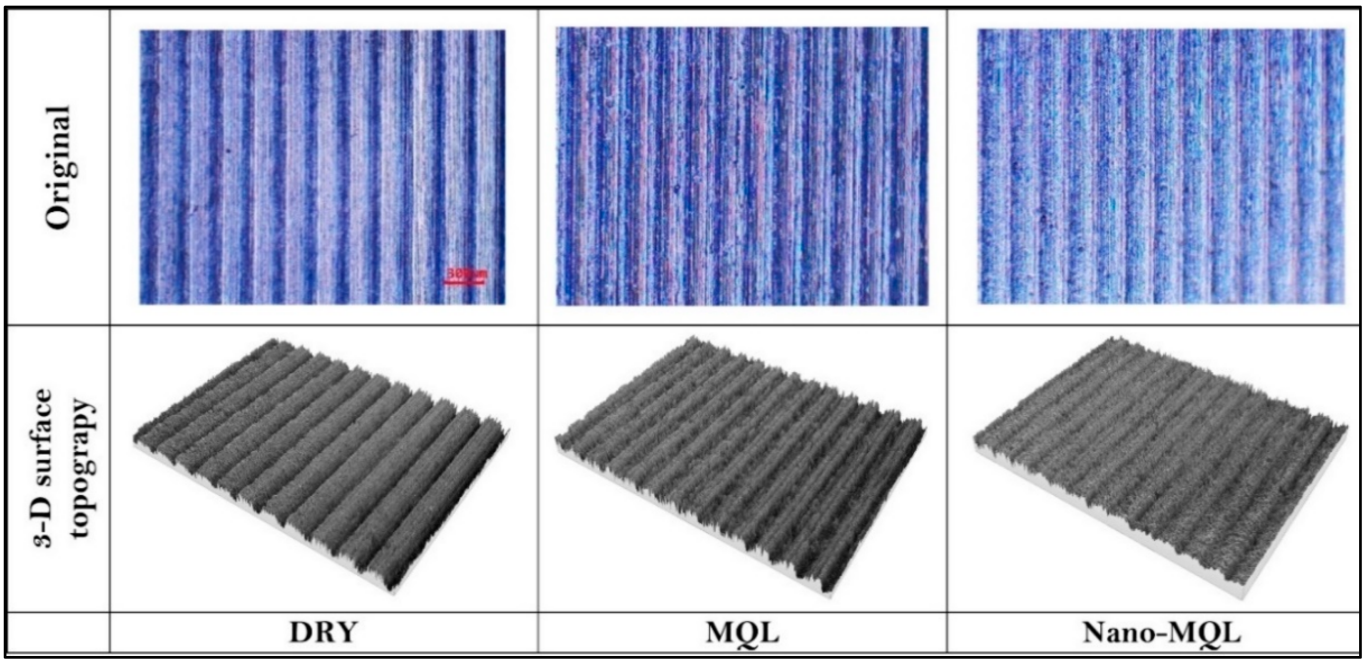

Figure 6. Surface roughness in V_c = 300 m/min and f = 0.15 mm/rev.

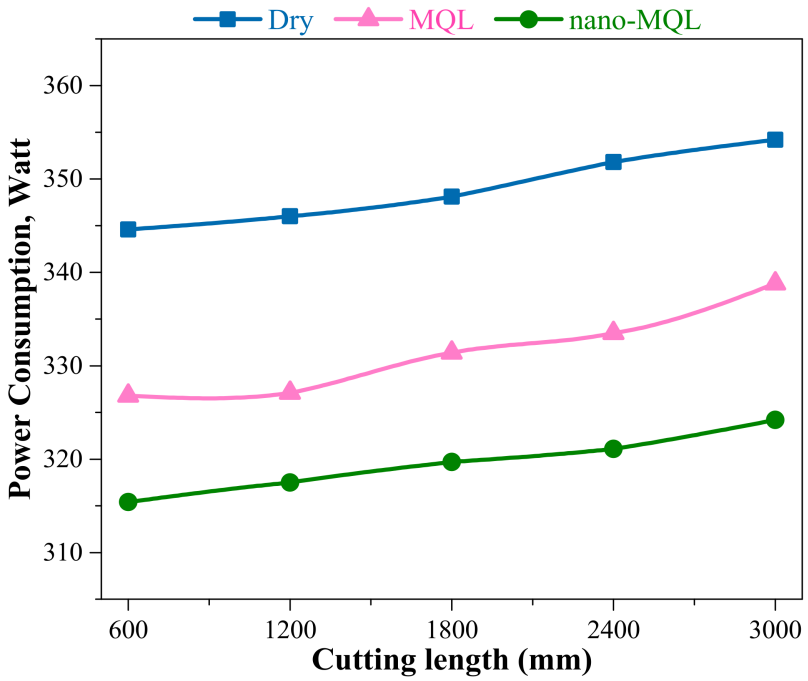

Figure 7. Variable of power consumption in V_c = 300 m/min and f = 0.15 mm/rev.

The energy required for chip removal is converted into heat in the cutting zone and that cannot be ignored. While the temperature is mostly formed at the cutting tool–chip interface, some of it is transmitted to the part. This affects the surface integrity of the machined surface as well as the cutting tool life. The temperature values measured as a result of the experiments are given in Figure 8. Similar trends and results were obtained at the cutting temperature as in other machining outputs. The highest temperatures were measured under dry cutting conditions, as expected. Based on the first stage measurements, the highest temperature was approximately 90 °C in dry cutting conditions. For MQL, the measurement taken at the same step was obtained at a 5% lower value. For nano-MQL, this ratio was approximately 14% less. For MQL and nano-MQL, this decreasing rate continues to increase at every stage. When it comes to the last stage, the temperature obtained under dry cutting conditions reached 170 °C. Under the same conditions, the decrease in MQL and nano-MQL was approximately 23.6% and 29.5%, respectively. These results affect the surface integrity and the amount of cutting tool wear, as mentioned above, and show a similar trend. As a result, it is seen that the MQL and nano-MQL systems have a positive effect on the temperature, as previously stated by Krolczyk et al. [45]. The thin layer and lubrication that MQL systems create in the cutting zone is the most important factor in reducing the cutting temperature. The fact that the nanoparticles added in addition to this system have good thermal conductivity, and evacuate the heat from the cutting zone faster, is the reason why the best results are obtained in nano-MQL. Figure 9 also shows the rise in temperature under dry cutting conditions in chip and shear development.

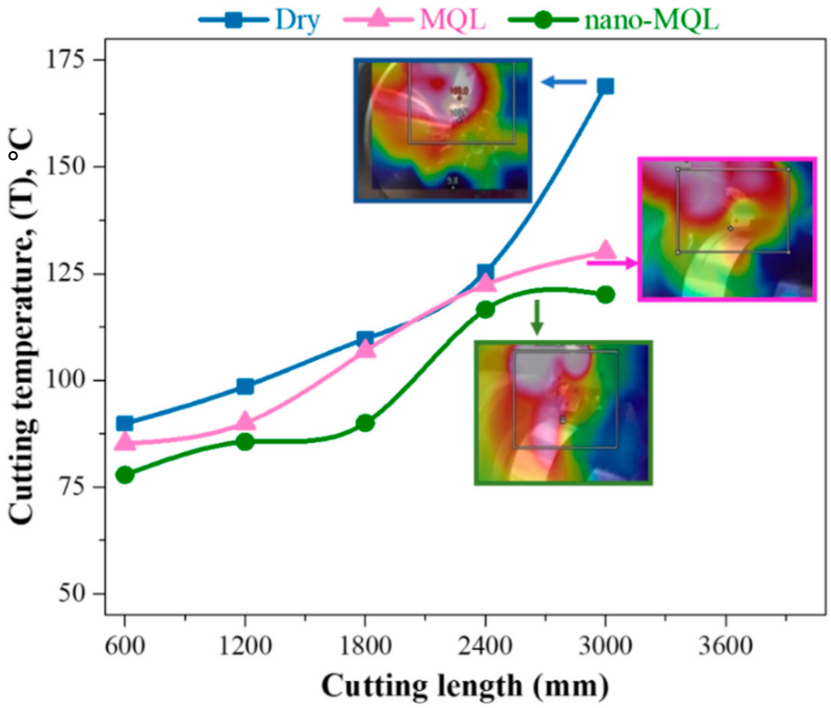

Figure 8. Variable of cutting temperature in V_c = 300 m/min and f = 0.15 mm/rev.

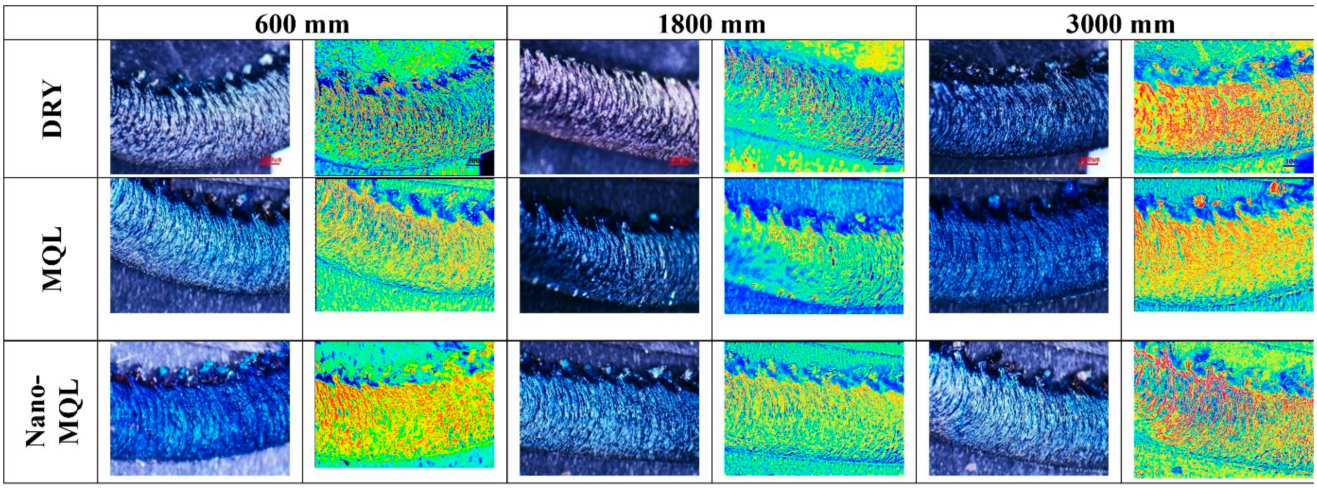

Figure 9. Variation of chip morphology in V_c = 300 m/min and f = 0.15 mm/rev.

4. Conclusions

The current study was conducted to evaluate the machinability of ER7 steel under dry, MQL and nano-MQL lubrication conditions. The aim was to determine the effect of using MQL cooling technologies and cutting parameters on the resulting machining outputs: surface finish, energy consumption, machining temperatures and tool wear. The following results can be concluded from this study:

- It is seen that there is a decrease in Ra values depending on the increasing cutting speed, while, on the contrary, it exhibits an increase in cutting temperature and energy consumption. The feed rate caused an increase in all machining outputs depending on its increasing values.
- Preliminary experiments show that the best surface roughness values, the optimum parameter values, are obtained at 300 m/min and 0.15 mm/rev. The error value was obtained as 0.915%.

- The highest values of VB were obtained in dry machining conditions at all machining lengths. When the VB value was compared with other applications, considering the last stage (3000 mm), it outperformed MQL and nano-MQL implementations by approximately 34.1% and 37.6%, respectively.
- It is clear that the lubrication methods have a significant impact on obtaining better surface quality when compared to the dry machining conditions. In the first stage (600 mm) measurements, the highest Ra value was obtained as 1.05 µm under dry machining conditions. Compared to the same conditions, the result obtained with MQL was approximately 24% lower, and the result obtained with nano-MQL was approximately 34% lower.
- The highest power consumption for each stage occurred under dry machining conditions. Since the sum of the powers obtained for each length is taken into account, it has been calculated that there is approximately 5.3% and 10.2% lower power consumption in the experiments performed with MQL and nano-MQL, respectively.
- The highest temperatures were measured under dry cutting conditions, as expected. Based on the first stage (600 mm) measurements, the highest temperature value was measured as approximately 90 °C in dry cutting conditions. For MQL, the measurement taken at the same stage was 5% lower, while for nano-MQL this rate was approximately 14% lower.
- It is anticipated that this study will be useful to research and development centers in the machining and railway industries, particularly those focusing on improving cooling technologies in the machining of railway components.

Author Contributions: Conceptualization, M.E.K. and K.G.; methodology, N.Y.; investigation, K.Y.Ç. and N.Y.; resources, K.Y.Ç. and N.Y.; data curation, M.B. and R.D.; writing—original draft preparation, D.Y.P. and R.D.; writing—review and editing, M.E.K. and K.G.; visualization, M.E.K., K.G. and N.Y.; supervision, N.Y. All authors have read and agreed to the published version of the manuscript.

Funding: This research received no external funding.

Institutional Review Board Statement: Not applicable.

Informed Consent Statement: Not applicable.

Data Availability Statement: Data used in this work can be requested by contacting the first author.

Acknowledgments: Authors are thankful to Kardemir Inc. for the valuable support for this study.

Conflicts of Interest: The authors declare no conflict of interest.

References

1. Hu, Y.; Zhou, L.; Ding, H.H.; Lewis, R.; Liu, Q.Y.; Guo, J.; Wang, W.J. Microstructure evolution of railway pearlitic wheel steels under rolling-sliding contact loading. *Tribol. Int.* **2021**, *154*, 106685. [CrossRef]
2. Minicucci, D.J.; Fonseca, S.T.; Boas, R.L.V.; Goldenstein, H.; Mei, P.R. Development of Niobium Microalloyed Steel for Railway Wheel with Pearlitic Bainitic Microstructure. *Mater. Res.* **2019**, *22*, e20190324. [CrossRef]
3. Molyneux-Berry, P.; Davis, C.; Bevan, A. The Influence of Wheel/Rail Contact Conditions on the Microstructure and Hardness of Railway Wheels. *Sci. World J.* **2014**, *2014*, 209752. [CrossRef] [PubMed]
4. Akay, M.E.; Ridvanogullari, A. Optimisation of machining parameters of train wheel for shrink-fit application by considering surface roughness and chip morphology parameters. *Eng. Sci. Technol. Int. J.* **2020**, *23*, 1194–1207. [CrossRef]
5. Hu, Y.; Watson, M.; Maiorino, M.; Liang, Z.; Wang, W.; Ding, H.; Lewis, R.; Meli, E.; Rindi, A.; Liu, Q.Y.; et al. Experimental study on wear properties of wheel and rail materials with different hardness values. *Wear* **2021**, *477*, 203831. [CrossRef]
6. Hu, Y.; Zhou, L.; Ding, H.H.; Tan, G.X.; Lewis, R.; Liu, Q.Y.; Guo, J.; Wang, W.J. Investigation on wear and rolling contact fatigue of wheel-rail materials under various wheel/rail hardness ratio and creepage conditions. *Tribol. Int.* **2020**, *143*, 106091. [CrossRef]
7. Mazzù, A.; Ghidini, A.; Provezza, L.; Petrogalli, C.; Faccoli, M. Study of the damage induced by thermomechanical load in ER7 tread braked railway wheels. *Procedia Struct. Integr.* **2019**, *18*, 170–182. [CrossRef]
8. Giętka, T.; Ciechacki, K. Modeling of Railway Wheels Made of Austempered Ductile Iron. *Arch. Metall. Mater.* **2016**, *61*, 1833–1838. [CrossRef]

9. Ding, H.; Mu, X.; Zhu, Y.; Yang, W.; Xiao, Q.; Wang, W.; Liu, Q.; Guo, J.; Zhou, Z. Effect of laser claddings of Fe-based alloy powder with different concentrations of WS2 on the mechanical and tribological properties of railway wheel. *Wear* **2022**, *488–489*, 204174. [CrossRef]
10. Kaewunruen, S.; Ngamkhanong, C.; Lim, C.H. Damage and failure modes of railway prestressed concrete sleepers with holes/web openings subject to impact loading conditions. *Eng. Struct.* **2018**, *176*, 840–848. [CrossRef]
11. Walia, M.S.; Vernersson, T.; Lundén, R.; Blennow, F.; Meinel, M. Temperatures and wear at railway tread braking: Field experiments and simulations. *Wear* **2019**, *440–441*, 203086. [CrossRef]
12. Yurtkuran, H.; Korkmaz, M.E.; Günay, M. Modelling and optimization of the surface roughness in high speed hard turning with coated and uncoated CBN insert. *Gazi Univ. J. Sci.* **2016**, *29*, 987–995.
13. Erden, M.A.; Yaşar, N.; Korkmaz, M.E.; Ayvacı, B.; Nimel Sworna Ross, K.; Mia, M. Investigation of microstructure, mechanical and machinability properties of Mo-added steel produced by powder metallurgy method. *Int. J. Adv. Manuf. Technol.* **2021**, *114*, 2811–2827. [CrossRef]
14. Liang, Q.; Zhang, D.; Wu, W.; Zou, K. Methods and Research for Multi-Component Cutting Force Sensing Devices and Approaches in Machining. *Sensors* **2016**, *16*, 1926. [CrossRef]
15. Ross, N.S.; Mia, M.; Anwar, S.; Manimaran, G.; Saleh, M.; Ahmad, S. A hybrid approach of cooling lubrication for sustainable and optimized machining of Ni-based industrial alloy. *J. Clean. Prod.* **2021**, *321*, 128987. [CrossRef]
16. Ross, N.S.; Gopinath, C.; Nagarajan, S.; Gupta, M.K.; Shanmugam, R.; Kumar, M.S.; Boy, M.; Korkmaz, M.E. Impact of hybrid cooling approach on milling and surface morphological characteristics of Nimonic 80A alloy. *J. Manuf. Process.* **2022**, *73*, 428–439. [CrossRef]
17. Khanna, N.; Shah, P. Chetan Comparative analysis of dry, flood, MQL and cryogenic CO2 techniques during the machining of 15-5-PH SS alloy. *Tribol. Int.* **2020**, *146*, 106196. [CrossRef]
18. Baldin, V.; Rosa Ribeiro da Silva, L.; Houck, C.F.; Gelamo, R.V.; Machado, Á.R. Effect of Graphene Addition in Cutting Fluids Applied by MQL in End Milling of AISI 1045 Steel. *Lubricants* **2021**, *9*, 70. [CrossRef]
19. Sampaio, M.A.; Machado, Á.R.; Laurindo, C.A.H.; Torres, R.D.; Amorim, F.L. Influence of minimum quantity of lubrication (MQL) when turning hardened SAE 1045 steel: A comparison with dry machining. *Int. J. Adv. Manuf. Technol.* **2018**, *98*, 959–968. [CrossRef]
20. Danish, M.; Gupta, M.K.; Rubaiee, S.; Ahmed, A.; Korkmaz, M.E. Influence of hybrid Cryo-MQL lubri-cooling strategy on the machining and tribological characteristics of Inconel 718. *Tribol. Int.* **2021**, *163*, 107178. [CrossRef]
21. Abrão, B.S.; Pereira, M.F.; da Silva, L.R.; Machado, Á.R.; Gelamo, R.V.; de Freitas, F.M.; Mia, M.; da Silva, R.B. Improvements of the MQL Cooling-Lubrication Condition by the Addition of Multilayer Graphene Platelets in Peripheral Grinding of SAE 52100 Steel. *Lubricants* **2021**, *9*, 79. [CrossRef]
22. Obikawa, T.; Kamata, Y.; Shinozuka, J. High-speed grooving with applying MQL. *Int. J. Mach. Tools Manuf.* **2006**, *46*, 1854–1861. [CrossRef]
23. Diniz, A.E.; Ferreira, J.R.; Filho, F.T. Influence of refrigeration/lubrication condition on SAE 52100 hardened steel turning at several cutting speeds. *Int. J. Mach. Tools Manuf.* **2003**, *43*, 317–326. [CrossRef]
24. Dhar, N.R.; Islam, M.W.; Islam, S.; Mithu, M.A.H. The influence of minimum quantity of lubrication (MQL) on cutting temperature, chip and dimensional accuracy in turning AISI-1040 steel. *J. Mater. Process. Technol.* **2006**, *171*, 93–99. [CrossRef]
25. Mia, M.; Gupta, M.K.; Singh, G.; Królczyk, G.; Pimenov, D.Y. An approach to cleaner production for machining hardened steel using different cooling-lubrication conditions. *J. Clean. Prod.* **2018**, *187*, 1069–1081. [CrossRef]
26. Khanna, N.; Shah, P.; Sarikaya, M.; Pusavec, F. Energy consumption and ecological analysis of sustainable and conventional cutting fluid strategies in machining 15–5 PHSS. *Sustain. Mater. Technol.* **2022**, *32*, e00416. [CrossRef]
27. Sen, B.; Gupta, M.K.; Mia, M.; Pimenov, D.Y.; Mikołajczyk, T. Performance Assessment of Minimum Quantity Castor-Palm Oil Mixtures in Hard-Milling Operation. *Materials* **2021**, *14*, 198. [CrossRef]
28. Dubey, V.; Sharma, A.K.; Vats, P.; Pimenov, D.Y.; Giasin, K.; Chuchala, D. Study of a Multicriterion Decision-Making Approach to the MQL Turning of AISI 304 Steel Using Hybrid Nanocutting Fluid. *Materials* **2021**, *14*, 7207. [CrossRef]
29. Gupta, M.K.; Khan, A.M.; Song, Q.; Liu, Z.; Khalid, Q.S.; Jamil, M.; Kuntoğlu, M.; Usca, Ü.A.; Sarıkaya, M.; Pimenov, D.Y. A review on conventional and advanced minimum quantity lubrication approaches on performance measures of grinding process. *Int. J. Adv. Manuf. Technol.* **2021**, *117*, 729–750. [CrossRef]
30. Yıldırım, Ç.V.; Sarıkaya, M.; Kıvak, T.; Şirin, Ş. The effect of addition of hBN nanoparticles to nanofluid-MQL on tool wear patterns, tool life, roughness and temperature in turning of Ni-based Inconel 625. *Tribol. Int.* **2019**, *134*, 443–456. [CrossRef]
31. Şirin, Ş.; Sarıkaya, M.; Yıldırım, Ç.V.; Kıvak, T. Machinability performance of nickel alloy X-750 with SiAlON ceramic cutting tool under dry, MQL and hBN mixed nanofluid-MQL. *Tribol. Int.* **2021**, *153*, 106673. [CrossRef]
32. Nguyen, T.K.; Do, I.; Kwon, P. A tribological study of vegetable oil enhanced by nano-platelets and implication in MQL machining. *Int. J. Precis. Eng. Manuf.* **2012**, *13*, 1077–1083. [CrossRef]
33. Şirin, Ş.; Kıvak, T. Performances of different eco-friendly nanofluid lubricants in the milling of Inconel X-750 superalloy. *Tribol. Int.* **2019**, *137*, 180–192. [CrossRef]
34. Talib, N.; Rahim, E.A. Performance of modified jatropha oil in combination with hexagonal boron nitride particles as a bio-based lubricant for green machining. *Tribol. Int.* **2018**, *118*, 89–104. [CrossRef]

35. Kim, J.S.; Kim, J.W.; Kim, Y.C.; Lee, S.W. Experimental Study on Environmentally-Friendly Micro End-Milling Process of Ti-6Al-4V Using Nanofluid Minimum Quantity Lubrication With Chilly Gas. In *AIn International Manufacturing Science and Engineering Conference*; American Society of Mechanical Engineers: New York, NY, USA, 2016.
36. Wang, Y.; Li, C.; Zhang, Y.; Yang, M.; Li, B.; Dong, L.; Wang, J. Processing Characteristics of Vegetable Oil-based Nanofluid MQL for Grinding Different Workpiece Materials. *Int. J. Precis. Eng. and Manuf.-Green Technol.* **2018**, *5*, 327–339. [CrossRef]
37. Sarkar, J. A critical review on convective heat transfer correlations of nanofluids. *Renew. Sustain. Energy Rev.* **2011**, *15*, 3271–3277. [CrossRef]
38. Pandey, K.; Datta, S. Chapter Eight—Machinability study of Inconel 825 superalloy under nanofluid MQL: Application of sunflower oil as a base cutting fluid with MWCNTs and nano-Al2O3 as additives. In *Sustainable Manufacturing and Design*; Kumar, K., Zindani, D., Davim, P., Eds.; Woodhead Publishing: Sawston, UK, 2021; pp. 151–197. ISBN 978-0-12-822124-2.
39. Chetan; Ghosh, S.; Rao, P.V. Comparison between sustainable cryogenic techniques and nano-MQL cooling mode in turning of nickel-based alloy. *J. Clean. Prod.* **2019**, *231*, 1036–1049. [CrossRef]
40. Korkmaz, M.E.; Günay, M. Experimental and Statistical Analysis on Machinability of Nimonic80A Superalloy with PVD Coated Carbide. *Sigma J. Eng. Nat. Sci.* **2018**, *36*, 1141–1152.
41. Țîțu, A.M.; Sandu, A.V.; Pop, A.B.; Țîțu, Ș.; Frățilă, D.N.; Ceocea, C.; Boroiu, A. Design of Experiment in the Milling Process of Aluminum Alloys in the Aerospace Industry. *Appl. Sci.* **2020**, *10*, 6951. [CrossRef]
42. Dyl, T. The designation degree of tool wear after machining of the surface layer of duplex stainless steel. *Materials* **2021**, *14*, 6425. [CrossRef]
43. Sun, S.; Brandt, M.; Dargusch, M.S. Machining Ti–6Al–4V alloy with cryogenic compressed air cooling. *Int. J. Mach. Tools Manuf.* **2010**, *50*, 933–942. [CrossRef]
44. Mohana Rao, G.; Dilkush, S.; Sudhakar, I.; Anil babu, P. Effect of Cutting Parameters with Dry and MQL Nano Fluids in Turning of EN-36 Steel. *Mater. Today Proc.* **2021**, *41*, 1182–1187. [CrossRef]
45. Krolczyk, G.M.; Maruda, R.W.; Krolczyk, J.B.; Wojciechowski, S.; Mia, M.; Nieslony, P.; Budzik, G. Ecological trends in machining as a key factor in sustainable production—A review. *J. Clean. Prod.* **2019**, *218*, 601–615. [CrossRef]
46. Sharma, V.S.; Dogra, M.; Suri, N.M. Cooling techniques for improved productivity in turning. *Int. J. Mach. Tools Manuf.* **2009**, *49*, 435–453. [CrossRef]
47. Yıldırım, Ç.V. Investigation of hard turning performance of eco-friendly cooling strategies: Cryogenic cooling and nanofluid based MQL. *Tribol. Int.* **2020**, *144*, 106127. [CrossRef]
48. Cetin, M.H.; Kabave Kilincarslan, S. Effects of cutting fluids with nano-silver and borax additives on milling performance of aluminium alloys. *J. Manuf. Process.* **2020**, *50*, 170–182. [CrossRef]
49. Kumar Gupta, M.; Boy, M.; Erdi Korkmaz, M.; Yaşar, N.; Günay, M.; Krolczyk, G.M. Measurement and analysis of machining induced tribological characteristics in dual jet minimum quantity lubrication assisted turning of duplex stainless steel. *Measurement* **2022**, *187*, 110353. [CrossRef]
50. Korkmaz, M.E.; Gupta, M.K.; Boy, M.; Yaşar, N.; Krolczyk, G.M.; Günay, M. Influence of duplex jets MQL and nano-MQL cooling system on machining performance of Nimonic 80A. *J. Manuf. Process.* **2021**, *69*, 112–124. [CrossRef]